

## Detection of SARS-CoV-2 and Its Related Factors on the Mucosal Epithelium of the Tongue

**Jun Tamiya<sup>1</sup>, Wakako Sakaguchi<sup>1</sup>, Kimiko Nakagawa<sup>2</sup>, Toshiharu Yamamoto<sup>3</sup>,  
Juri Saruta<sup>4</sup>, Nobuhisa Kubota<sup>5</sup>, Akira Kawata<sup>1</sup>, Iwao Hasegawa<sup>2</sup>, Nobushiro Hamada<sup>6</sup>  
and Keiichi Tsukinoki<sup>1</sup>**

<sup>1</sup>Department of Pathology and Histomorphology, Kanagawa Dental University, 82 Inaoka, Yokosuka, Kanagawa 238–8580, Japan, <sup>2</sup>Department of Forensic Medicine, Kanagawa Dental University, 82 Inaoka, Yokosuka, Kanagawa 238–8580, Japan, <sup>3</sup>Department of Dentistry, Kanagawa Dental University, 82 Inaoka, Yokosuka, Kanagawa 238–8580, Japan, <sup>4</sup>Department of Education Planning, Kanagawa Dental University, 82 Inaoka, Yokosuka, Kanagawa 238–8580, Japan, <sup>5</sup>Department of Diagnostic Pathology, Kanagawa Dental University, 82 Inaoka, Yokosuka, Kanagawa 238–8580, Japan and <sup>6</sup>Department of Oral Microbiology, Kanagawa Dental University, 82 Inaoka, Yokosuka, Kanagawa 238–8580, Japan

Received October 10, 2022; accepted December 13, 2022; published online April 8, 2023

SARS-CoV-2 infects a variety of tissues, including the oral cavity. However, there are few reports examining the association of SARS-CoV-2 with tongue mucosal tissues with sticky tongue debris. This study investigated the presence of SARS-CoV-2 and its associated molecules by dissecting tongue tissue from autopsy specimens of 23 patients who died of COVID-19-related illness (pneumonia). Immunohistochemical staining, electron microscopy, and PCR analysis were performed on the tongue tissue specimens. The mucosal epithelium of the tongue formed a very thick keratinized with well-developed filiform papillae in all cases. ACE2 and TMPRSS2 were consistently co-expressed in all samples in the epithelium. The S-protein was strongly expressed in basal cells and the epithelial surface. S-protein-positive viral particles were detected in the tongue's stratified squamous epithelium via an immunoelectron microscope. Based on PCR amplification of the N1 and N2 regions, the SARS-CoV-2 gene was detected on the tongue epithelium, tongue submucosa, and in tongue debris. This suggests that tongue debris, including the squamous epithelial tissue, could be a source of SARS-CoV-2 in saliva. Furthermore, removing tongue debris may decrease the amount of SARS-CoV-2 in the oral cavity.

**Key words:** SARS-CoV-2, tongue debris, spike protein, autopsy case

### I. Introduction

The coronavirus disease 2019 (COVID-19) is an emerging infectious disease caused by SARS-CoV-2 that primarily infects the respiratory mucosa leading to symptoms ranging from asymptomatic to fatal [18]. The severe acute respiratory syndrome-associated coronavirus-2 (SARS-CoV-2) has a projecting appearance and contains a

spike protein (S-protein) that is critical for infection [6]. The S-protein comprises a receptor binding domain (RBD) in Supplemental Fig. S1 and a membrane fusion site in Supplemental Fig. S2 [18]. It has been suggested that angiotensin-converting enzyme 2 (ACE2) is the primary receptor for SARS-CoV-2 because the S1-RBD of this virus binds to ACE2 *in vivo* [4].

COVID-19 is diagnosed using saliva, nasal swabs, and pharyngeal swabs; however, saliva specimens are primarily used in Japan owing to their advantages in infection control [9]. Saliva is a complex liquid consisting of salivary gland secretions, cellular components of the oral cavity (including

Correspondence to: Wakako Sakaguchi, Department of Pathology and Histomorphology, Kanagawa Dental University, 82 Inaoka, Yokosuka, Kanagawa 238–8580, Japan. E-mail: sakaguchi@kdu.ac.jp

**Table 1.** *Antibodies used for immunostaining*

Antibody	Clone	Supplier	Dilution for IHC	Retorival
ACE2	HPA000288	Sigma-Aldrich, MO, USA	500	Citrate buffer (pH6)
TMPRSS2	ab92323	Abcam, Cambridge, UK	1000	Tris-EDTA (pH9)
S-protein	3525	ProSci, CA, USA	2000	Tris-EDTA (pH9)
Ki67	MIB-1	Dako, CA, USA	Diluted	Citrate buffer (pH6)

exfoliated epithelial cells), and respiratory tract secretions; therefore, the origin of the virus in saliva is diverse.

Using single-cell RNA-seq profiling, a report published in February 2020 revealed that ACE2 expression in oral tissues was higher in the tongue than in buccal or gingival tissue [22]. This was the first report identifying the association between SARS-CoV-2 and the oral cavity [22]. However, up to the SARS-CoV-2 delta strain, the route of entry into the organism required activation of S2 membrane fusion via the transmembrane serine protease 2 (TMPRSS2) [19]; thus, cells co-expressing ACE2 and TMPRSS2 were considered to be at high risk of infection [3].

The presence of ACE2 and TMPRSS2 in oral mucosal epithelial tissue, as revealed by immunohistochemical analysis of oral mucosa (including the tongue mucosa), suggested that the oral mucosa could be a target for SARS-CoV-2 [16]. In addition, a study published in March 2021 reported the presence of SARS-CoV-2-infected oral mucosal cells in saliva, confirming that the oral cavity is a crucial SARS-CoV-2 infection site [8].

Although SARS-CoV-2 has been shown to infect the salivary glands [11] and gingiva [12], there have been no reports of infection of the tongue mucosa. The presence of TMPRSS2 on the tongue has been linked to an increased risk of SARS-CoV-2 infection [16]. The presence of bacteria, food residues, and exfoliated epithelium in tongue debris suggests that the tongue could serve as a SARS-CoV-2 source. The study aimed to evaluate the expression of infection-promoting factors in the tongue mucosa of COVID-19-related autopsy specimens. Determining the localization of SARS-CoV-2 on the tongue mucosa can lead to a better understanding of the virus profile in saliva and development of a novel diagnostic strategy that is simpler and less likely to cause droplet infection than conventional methods. It would also demonstrate the importance of oral care as a countermeasure against SARS-CoV-2.

## II. Materials and Methods

### Cases

Twenty-three of twenty-nine autopsy cases with suspected COVID-19-related death were examined at the Kanagawa Autopsy Center affiliated with Kanagawa Dental University from May 17 to October 14, 2021. The 23 cases consisted of 17 males and 6 females, with age ranging from 46 to 90 years (mean age: 66.6 years). The mean time from the date of death to the date of autopsy was 3.4

days, ranging from 1 to 14 days. The primary cause of death was severe pneumonia. Twenty-three cases with positive PCR results for SARS-CoV-2 were used for immunohistochemical analysis. Eleven cases were used for PCR analysis, and one was used for electron microscopy analysis. This study was reviewed and approved by the Kanagawa Dental University Research Ethics Review Committee (No. 734).

### Specimen processing

The posterior one-third of the tongue was excised as the main collection site during the autopsy to include as much of the vallate papilla as possible. The specimens were fixed in 10% formalin solution for at least 24 hr and then refixed in 95% ethanol solution at 22°C for at least 24 hr. Paraffin-embedded blocks were prepared, and unstained sections were used for Hematoxylin & eosin staining (H&E staining) and immunostaining (Table 1). RNA was extracted from formalin-fixed specimens for PCR experiments.

### Immunostaining

Thin 4  $\mu\text{m}$  thickness were mounted and deparaffinized. To remove peroxidase, the sections were incubated with 3% hydrogen peroxide (Wako, Osaka, Japan) for 30 min. The sections were then treated for antigen retrieval (Table 1). Primary antibodies were incubated at 4°C for 17 hr. Secondary antibodies were incubated with the Histofine PO-M kit (Nichirei, Tokyo, Japan) for 10 min at room temperature. The antibodies were then stained with 3,3'-diaminobenzidine (DAB, Wako) and sealed after nuclear staining. Negative controls were reacted with PBS instead of the primary antibody. As negative control, tongue tissues from patients who died before the pandemic, were used.

### Immunoelectron microscopy

Immunoelectron microscopy was performed according to our previous studies [10, 20]. For the pre-embedding method, samples fixed in 10% formalin were immersed in 20% sucrose and cut into 50  $\mu\text{m}$ -thick sections using a sliding microtome (Leica, Wetzlar, Germany) equipped with a freezing stage. The sections were then treated with 1% borohydride for 10 min, washed with PBS for 1 hr, and non-specific protein binding was blocked using 2% bovine serum albumin (BSA) in PBS. The sections were then incubated with 1:2000 diluted anti-S protein serum antibody (ProSci, CA, USA) in PBS containing 1% BSA and 0.1% Tween 20 (PBS-BSAT) for 1 day at 4°C. After

rinsing in PBS for 1 hr, the sections were incubated with biotinylated anti-rabbit IgG (BA-1000; Vector Laboratories, Burlingame, CA, USA) diluted to 1:100 in PBS-BSAT solution for 1 hr at 22°C. The sections were then washed again in PBS and incubated with avidin-biotin-horseradish peroxidase complex (PK-6100; Vector Laboratories, CA, USA) diluted to 1:200 in PBS-BSAT for 30 min at 22°C. After a final wash in PBS, the sections were reacted with 0.02% DAB and 0.005% hydrogen peroxide in 0.05 M Tris-HCl buffer solution (pH 7.4) for 5 min. After rinsing in PBS, the sections were treated with 2% OsO<sub>4</sub> in PB (pH 7.4) for 1 hr at 22°C, dehydrated by graded alcohol solution, cleared in propylene oxide, and embedded in Quetol 812 (Nissin EM, Tokyo, Japan). Subsequently, ultrathin sections were obtained and mounted on nickel grids (Nissin EM.). After staining with lead citrate for 1 min [15], the sections were examined under an H-7600 transmission electron microscope (Hitachi High Technology, Tokyo, Japan).

#### ***Collection of the tongue surface, epithelial tissue, and subepithelial tissue and RNA extraction***

The superficial layer of the tongue mucosa was abraded with a tongue cleaner (Shonan Medical, Kanagawa, Japan), and the superficial layer, including the tongue coating, was collected. The specimens from which the superficial layer was removed were observed under a fact microscope, and only the squamous epithelium was harvested using a scalpel. In addition, the subepithelial tissue was collected by excising the area just below the epithelium with a scalpel. The collected specimens were immersed in 100% ethanol solution.

RNA extraction was performed using the FFPE RNA purification kit (Norgen Biotek, Toronto, Canada) according to the customary method. Samples were dissolved by adding proteinase K, and lysates were prepared by adding 100% ethanol. After passing the lysate through the column, DNase and enzyme incubation buffer A were added. Wash solution A was then added to wash the column. Next, elution solution A was added to the column and centrifuged to extract RNA. The purity of the extracted RNA was confirmed using an absorbance spectrophotometer.

#### ***Detection of SARS-CoV-2 mRNA***

The extracted RNA was standardized to a concentration of 100 ng/μL and used for PCR. All of the manufacturer's instructions were followed for the detection of SARS-CoV-2 mRNA, except for the Ampdirect TM 2019-nCoV detection kit (Shimadzu, Chukyou, Kyoto), which was modified. [Available from: <https://www.cdc.gov/coronavirus/2019-ncov/lab/rt-pcrpanel-primer-probes.html>] (accessed on April 2 2022). Namely, PCR reactions were performed using separate primers for N1, N2, and IC. Melting analysis was typically performed to confirm the specificity of the PCR products; however, the PCR products of N1, N2, and IC were applied to a 1% agarose gel

containing ethidium bromide and electrophoresed without melting analysis. Tongue debris from SARS-CoV-2 PCR-negative individuals were used as negative controls. A LightCycler480® (Roche, Basel, Switzerland) thermal cycler was used for the PCR reactions. Extracted RNA was evaluated by amplification of the human RNase P gene, and appropriate samples were tested for SARS-CoV-2 by real-time PCR (RT-PCR).

#### ***Statistical analysis***

Tongue samples were separated into three parts: tongue surface, stratified squamous epithelium, and subepithelial tissue. Ct values were compared by one-way analysis of variance after equal variance was confirmed by the Barlett test. The significance level was set at 5%. All analyses were performed using the statistical software package Statcel4 (OMS, Tokyo, Japan).

#### ***Institutional review board statement***

This study was reviewed by the Kanagawa Dental University Research Ethics Review Committee and approved No. 734.

#### ***Informed consent statement***

Patient consent was waived due to the fact that the study was performed on cadavers.

### **III. Results**

#### ***Morphological findings***

The mucosal epithelium of the tongue formed a very thick keratinized with well-developed filiform papillae (Fig. 1A). The histology resembled that of a black, hairy tongue. The superficial layer of the squamous epithelium showed marked keratinization, bacterial adherence and exfoliated cells, but no granular cell was formed (Fig. 1B). The cytoplasm of the cells in the stratum spinosum contained cells showing vacuolation and paling (Fig. 1C). The basal cell showed no increase in mitosis. Some cells showed a bright zone suggesting an inclusion body-like structure. No atypia was observed in the squamous epithelium of the tongue.

#### ***Immunohistochemical findings***

ACE2 was consistently expressed in all samples in the epithelium (Fig. 2A). There were some scattered cells with higher expression than the surrounding cells (Fig. 2B). ACE2 was localized at the plasma membrane and in the cytoplasm. TMPRSS2 was mainly localized in the plasma membrane of the epithelium and was expressed in the epithelium (containing the stratum corneum and the tongue debris) of all 23 samples (Fig. 3A). ACE2 and TMPRSS2 were co-expressed in the epithelium (Fig. 2A, B, Fig. 3B, C), and S-protein (a specific SARS-CoV-2 antigen) was expressed in the basal cells and epithelial surface (Fig. 4A: 100% of the epithelial layers, 23/23). The obvious S-

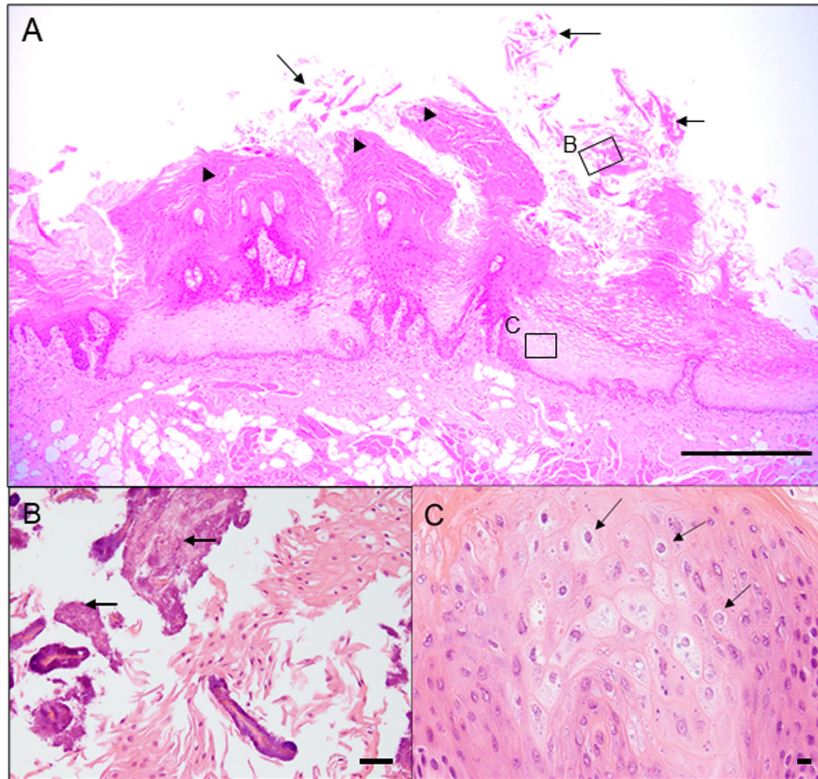


**Fig. 1.** (A) Hematoxylin & eosin staining (H&E staining) of the dorsum of the tongue from SARS-CoV-2-positive postmortem specimen. Bar = 200  $\mu$ m. Tongue mucosal epithelium was thickly keratinized and exhibited well-developed filiform papillae (A; arrowhead). In addition, adherent and shed-ding bacterial cells were observed (B; arrows); Bar = 50  $\mu$ m; cytoplasmic inclusion body structures (C; arrows), and vacuolation were observed in stratum spinosum cells; Bar = 20  $\mu$ m.

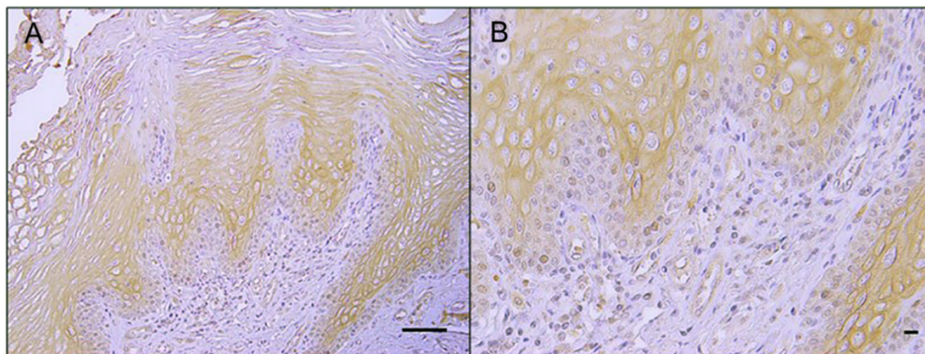


**Fig. 2.** Immunohistochemical findings for SARS-CoV-2 related protein in the epithelial of the dorsal tongue. Staining with ACE2 antibody. Bar = 50  $\mu$ m (A), Bar = 20  $\mu$ m (B). Figures 2, 3, 4, and 6 represent sequential sections of the same sample from SARS-CoV-2-positive postmortem specimen.

protein-positive cells were capillary epithelial cells in the subepithelial tissue (Fig. 4C). Cytoplasm inclusion bodies were observed in some cells showing high expression (Fig. 4B). In contrast, no S-protein was observed in the pre-pandemic tongue samples (Fig. 5). In both cases, Ki-67-positive cells were observed in the nuclei of the basal and parabasal (Fig. 6).

#### **Electron microscopy and immunoelectron microscopy**

The immune-positive DAB deposition of S protein was detected in electron micrographs as the densest fine

structure (Fig. 7, arrows). The immunoreactive DAB deposition of S protein was seen in restricted ribosomal clusters within cells (Fig. 7, black arrows) and was distinguished from immune-negative ribosomes with low electron density (Fig. 7, dotted arrows). These DAB-deposited ribosomes were found in both tongue glands and stratified squamous epithelium of the tongue. In the lingual glands, these immunoreactive ribosomal clusters were observed in cells comprising the secretory ducts (Fig. 7, image enlargement). In addition, these profiles were also observed in squamous epithelium, which is characterized by the presence of com-

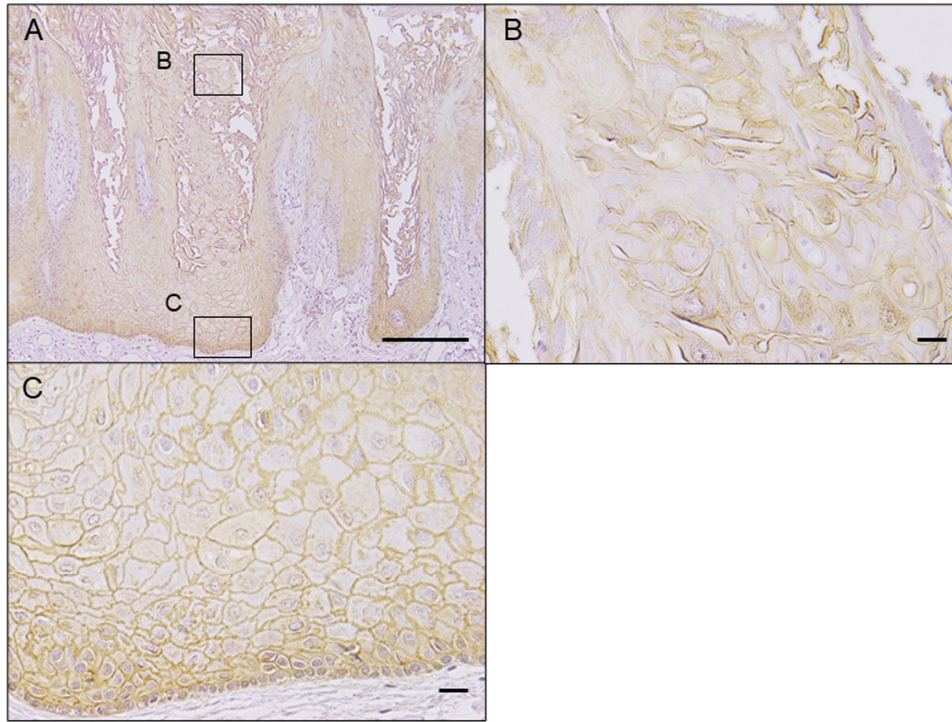


**Fig. 3.** (A) Immunohistochemical findings for SARS-CoV-2 related protein in the epithelial of the dorsal tongue. Staining with TMPRESS2 antibody. Bar = 100  $\mu$ m. (B) Magnified view of stratum corneum of tongue. Bar = 20  $\mu$ m. (C) Magnified view of the basement membrane layer of the tongue. Bar = 20  $\mu$ m. Figures 2, 3, 4, and 6 represent sequential sections of the same sample from SARS-CoV-2-positive postmortem specimen.

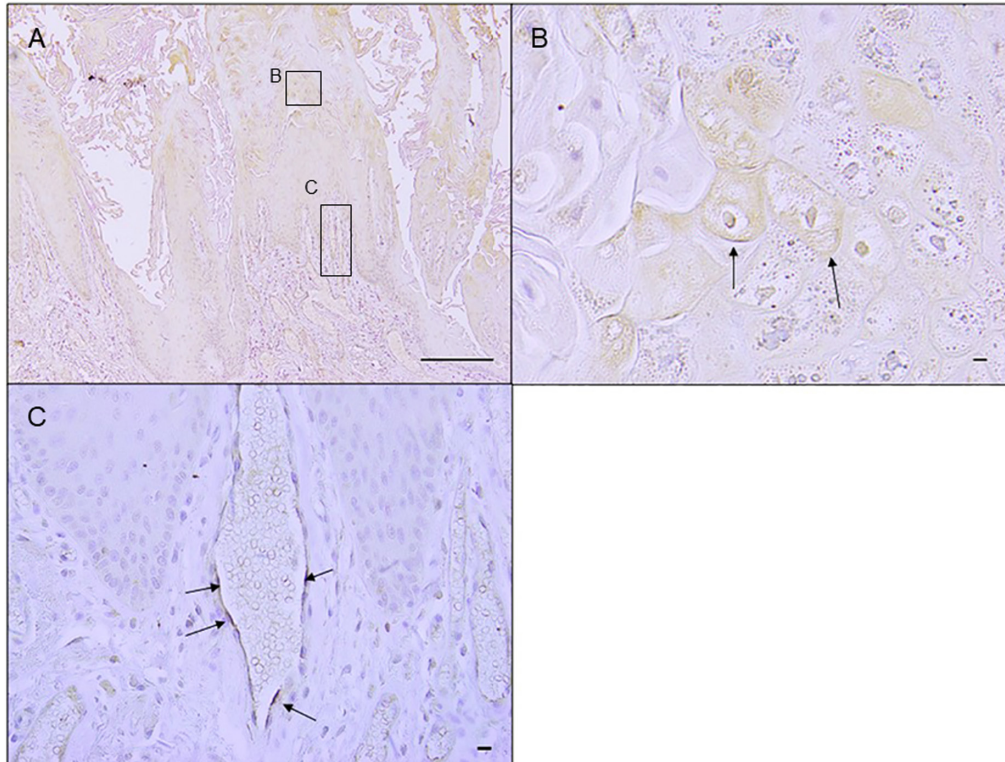


**Fig. 4.** (A) Immunohistochemical findings for SARS-CoV-2 related protein in the epithelial of the dorsal tongue. Staining with S-protein antibody. Bar = 100  $\mu$ m. (B) Arrows indicate positive areas of epithelial cell cytoplasm. Bar = 20  $\mu$ m. (C) Arrows indicate positive areas of vascular endothelial cells. Bar = 20  $\mu$ m. Figures 2, 3, 4, and 6 represent sequential sections of the same sample from SARS-CoV-2-positive postmortem specimen.

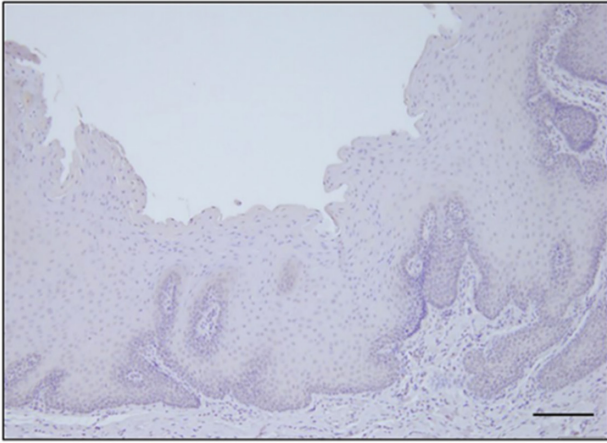


**Fig. 5.** Staining with S-protein antibody of the pre-pandemic sample. Bar = 100  $\mu$ m.

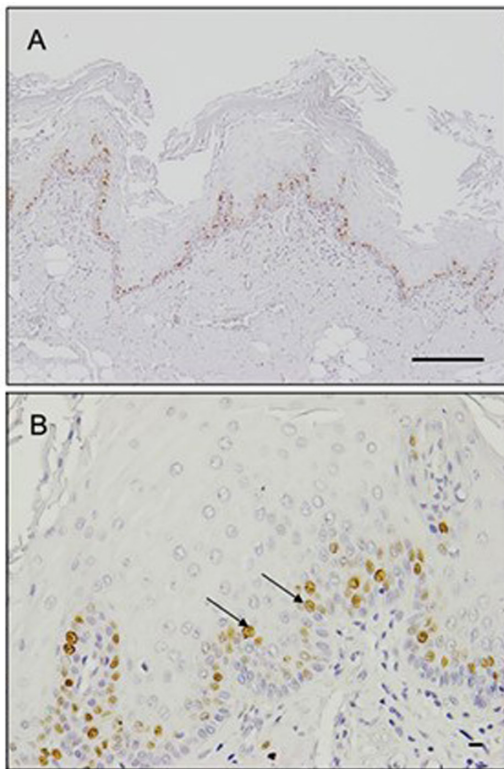


**Fig. 6.** (A) Staining with Ki-67 antibody for SARS-CoV-2-positive postmortem specimen. Staining of SARS-CoV-2 positive postmortem specimens with Ki-67 antibody. Bar = 100  $\mu$ m. (B) Ki-67-positive cells are indicated by arrows. Bar = 20  $\mu$ m. Figures 2, 3, 4, and 6 show consecutive sections of the same sample of SARS-CoV-2 positive postmortem specimens.

plex intercellular junctions (Fig. 8). Some immunoreactive ribosomal clusters formed circular structures 90–140 nm in diameter, suggesting a process of S-protein synthesis (Fig. 8, enlarged inset).

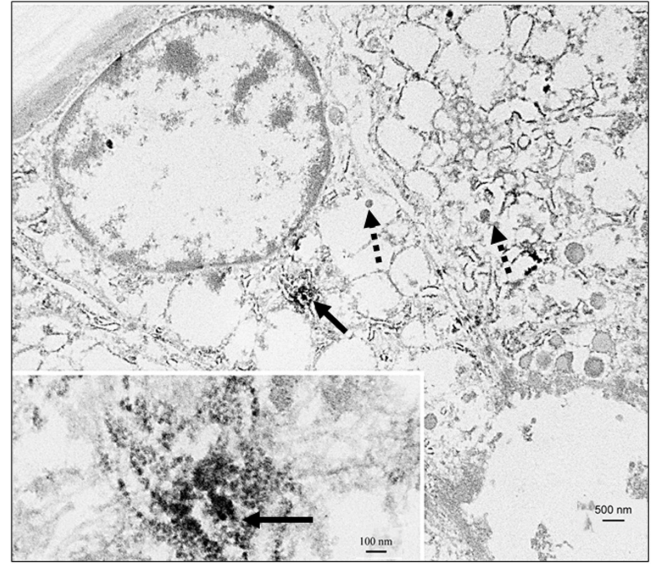


**Fig. 7.** Immunoelectron microscopy image of the minor salivary gland of the tongue mucosa S-protein. Bar = 500 nm, HV = 80.0 KV. Immune-positive depositions in the lingual glands on the dorsal surface of the tongue are indicated by black solid arrows; the immune-negative ribosomes with low electron density are indicated by black dotted arrows. Inset image magnified to 100 nm.

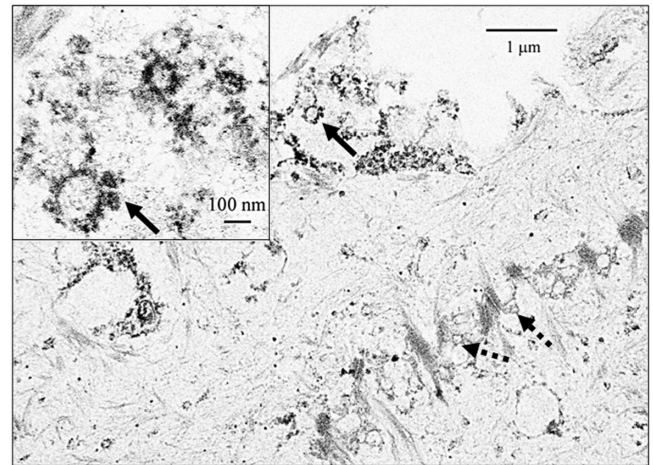


**Fig. 8.** Immunoelectron microscopy image of the epithelium of the tongue mucosa S protein. Immune-positive depositions are indicated by black solid arrows, while immune-negative ribosomes are indicated by black dotted arrows. Bar = 1  $\mu$ m. HV = 80.0 KV. Inset image magnified to 100 nm.

### PCR

There was positive PCR detection of N1 and N2 on the tongue surface, epithelium, and under the epithelium (Fig. 9A, B) in all COVID-19-positive cases (Fig. 9C, D). However, PCR analysis of the tongue surface of COVID-19-negative patients was negative for both N1 and N2 (Ct:0). The mean and standard error of N1 Ct values

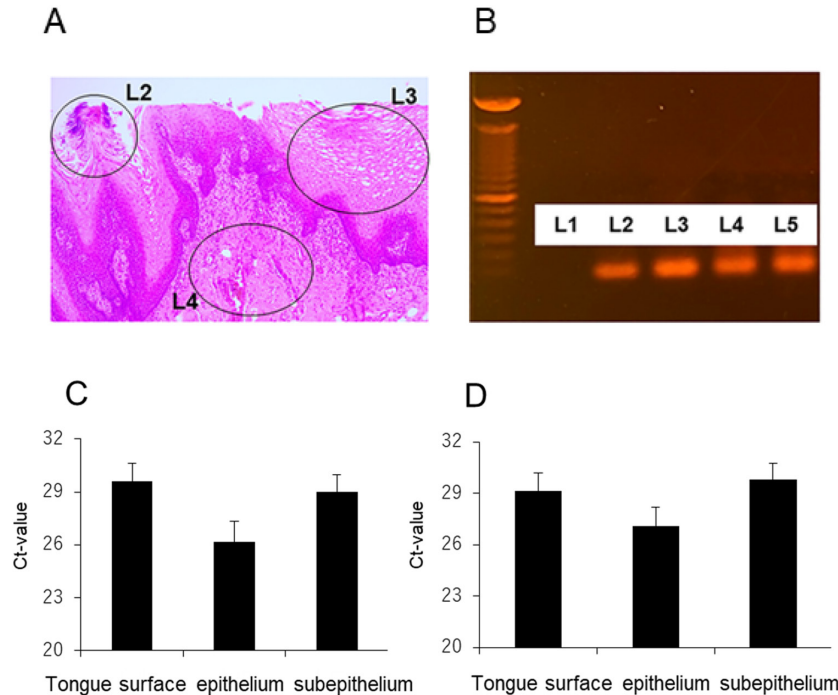


**Fig. 9.** PCR analysis for COVID-19 positive cases are shown. (A) H&E staining of SARS-CoV-2-positive case. (B) PCR image for N1. L1: negative control (SARS-CoV-2-negative tongue surface), L2: tongue surface (including bacteria, keratin, and some spicules), L3: tongue epithelium (after cut of surface), L4: beneath the epithelium (including the mucosa intrinsic, submucosa, and muscular), L5: internal control. (C) Polymerase chain reaction (PCR) analysis of N1. ( $n = 11$ ,  $p > 0.05$ ) (D) PCR analysis of N2. ( $n = 11$ ,  $p > 0.05$ ).

were  $29.13 \pm 1.08$  for the tongue surface,  $27.08 \pm 1.14$  for the epithelium, and  $29.79 \pm 0.96$  for under the epithelium, which were not significantly different. The mean and standard error of N2 Ct values were  $29.62 \pm 0.99$  for the tongue surface,  $14.75 \pm 1.16$  for the epithelium, and  $10.30 \pm 0.97$  for under the epithelium, which were not significantly different. RNase P was positive in all cases.

#### IV. Discussion

This study analyzed a portion of tongue tissue from SARS-CoV-2 positive postmortem specimens. There were no necrotic or degenerative changes observed, and proliferative activity was detected in the basal- and parabasal layers, indicating that the samples were not significantly affected by postmortem changes. Furthermore, there was no significant RNA degradation based on RNA purity and PCR analysis of RNase P despite the use of a formalin-fixed sample. Histochemical findings of marked keratinization on the surface of the tongue were common in all SARS-CoV-2 positive cases. Rajkumari *et al.* [14] reported nuclear swelling and cytoplasmic vacuolation in the tongue of autopsy cases without COVID-19 but no hyperkeratosis, and the same result was found in the gingiva [13]. In this study, we excised a sample of the gingival mucosa for histological observation and confirmed that there was no hyperkeratosis (data not shown). The observed proliferation

and thickening of keratin in the basal layer may be due to the fact that postmortem specimens unlikely shed surface cells as their tongues do not move. However, this is inconsistent with previous reports [21]. On the other hand, COVID-19 presents extensive cutaneous manifestations, but there are scattered case reports of skin disease showing hyperkeratosis. In addition, HE-stained images of tongue tissue from patients that died of COVID-19 showed increased tongue papillae and hyperkeratosis [7]. Future studies are needed to elucidate the mechanism of hyperkeratosis of the tongue mucosa in patients with COVID-19.

Sakaguchi *et al.* reported that ACE2 was localized in the basal- and spinous cell layer of the tongue-stratified squamous epithelium with strong expression in the epithelial surface [19]. ACE2 is strongly expressed in the upper one-third of the stratified squamous epithelium, and TMPRSS2 is localized in the plasma membrane of the spicule [17]. In this study, immunohistochemical localization showed ACE2 and TMPRSS2 expression in all layers of the stratified squamous epithelium, especially in the superficial layer of the epithelium, which was more extensive than in previous reports. This study used a COVID-19 death case, and there may be a difference in expression between infected cases and non-infected cases used in previous reports.

PCR amplification of the N1- and N2 regions showed positive reactions from the tongue surface, including

tongue debris, epithelium, and under the epithelium in all COVID-19-positive cases. Ct values were not significantly different between the tongue surface, epithelium, and under the epithelium. Previous studies reported the presence of SARS-CoV-2 RNA *in vivo* from formalin-fixed paraffin-embedded tongue squamous cell carcinoma and submandibular gland tissue [5]. Furthermore, real-time RT-PCR testing revealed the presence of SARS-CoV-2 RNA in tongue tissue from 6 of 8 patients who tested positive [2]. Tongue debris is a deposit on the tongue surface containing sloughed stratified squamous epithelium. The tongue surface, including tongue debris, epithelium and under the epithelium, contained comparable amounts of viral RNA. This suggests that tongue debris is a reservoir of virus-infected cells. This is the first report showing SARS-CoV-2 RNA in tongue debris by PCR.

The S-protein is a component of SARS-CoV-2 and is expressed in infected cells. The S-protein was immunohistochemically identified in the stratified squamous epithelium of the tongue mucosa. Furthermore, the S-protein was immunohistochemically positive for viral particles in the squamous epithelium of the tongue by transmission electron microscopy, and SARS-CoV-2 RNA was detected by PCR. This multifaceted verification of SARS-CoV-2 in the stratified squamous epithelium of the tongue confirmed that SARS-CoV-2 infects the epithelial tissue of the tongue.

The tongue samples used in this study were collected prior to the spread of the Omicron strain in Japan. It is suggested that the route of invasion differs between the Omicron strain and the earlier strains [17]. Further studies are needed to determine whether the Omicron strain exhibits the same sexual characteristics as the earlier prevalent strain.

Tongue debris increases the risk of pneumonia when aspirated into the airway; therefore, treatment of tongue coating during oral care is significant for its prevention [1]. This study showed the presence of SARS-CoV-2 on the tongue surface, indicating that it is one of the most potent sources of the virus in saliva. It is thought that the removal of tongue coating may also be potent in reducing viruses in the oral cavity, and oral care is expected to contribute to the countermeasure of SARS-CoV-2.

## V. Conclusions

The association between SARS-CoV-2 and the tongue mucosa using autopsy specimens was investigated. Electron microscopy and PCR analysis revealed that SARS-CoV-2 infects epithelial cells of the tongue mucosa, indicating that tongue tissue is one of the sources of SARS-CoV-2 in saliva. In particular, tongue debris is considered a source of SARS-CoV-2, and oral care is important as a countermeasure against SARS-CoV-2.

## VI. Conflicts of Interest

The authors declare that there are no conflicts of interest.

## VII. Funding

This work was funded by the Kanagawa Dental University Division of Pathology Research Funding FY 2021 From Kanagawa Dental University, Japan.

## VIII. Author Contributions

Conceptualization, methodology, W.S., T.Y., and K.T.; formal analysis, W.S.; validation, W.S., T.Y., and K.T. resources, K.N., I.H. investigation, J.T., W.S., T.Y., J.S., N.K., A.K. and N.H., writing—original draft preparation, J.T., W.S., T.Y., K.T. preparation Conceptualization, K.T. project administration, K.T.; funding acquisition, K.T. All authors have read and agreed to the published version of the manuscript.

## IX. Acknowledgments

We would like to thank the Kanagawa Dental University Graduate School Central Research Center for their support and Editage ([www.editage.com](http://www.editage.com)) for English language editing.

## X. References

1. Abe, S., Ishihara, K., Adachi, M. and Okuda, K. (2008) Tongue-coating as risk indicator for aspiration pneumonia in edentate elderly. *Arch. Gerontol. Geriatr.* 47; 267–275.
2. Butowt, R., Bilińska, K. and von Bartheld, C. (2022) Why does the Omicron variant largely spare olfactory function? Implications for the pathogenesis of anosmia in COVID-19. *J. Infect. Dis.* 226; 1304–1308.
3. Collin, J., Queen, R., Zerti, D., Dorgau, B., Georgiou, M., Djidrovski, I., *et al.* (2021) Co-expression of SARS-CoV-2 entry genes in the superficial adult human conjunctival, limbal and corneal epithelium suggests an additional route of entry via the ocular surface. *Ocul. Surf.* 19; 190–200.
4. Gao, X., Zhang, S., Gou, J., Wen, Y., Fan, L., Zhou, J., *et al.* (2022) Spike-mediated ACE2 down-regulation involved was in the pathogenesis of SARS-CoV-2 infection. *J. Infect.* 85; 418–427.
5. Guerini-Rocco, E., Taormina, S. V., Vacirca, D., Ranghiero, A., Rappa, A., Fumagalli, C., *et al.* (2020) SARS-CoV-2 detection in formalin-fixed paraffin-embedded tissue specimens from surgical resection of tongue squamous cell carcinoma. *J. Clin. Pathol.* 73; 754–757.
6. Hasan, A., Paray, B. A., Hussain, A., Qadir, F. A., Attar, F., Aziz, F. M., *et al.* (2020) A review on the cleavage priming of the spike protein on coronavirus by angiotensin-converting enzyme-2 and furin. *J. Biomol. Struct. Dyn.* 39; 3025–3033.
7. Henin, D., Pellegrini, G., Carmagnola, D., Attisano, G. C. L., Lopez, G., Ferrero, S., *et al.* (2022) Morphological and immunopathological aspects of lingual tissues in COVID-19.

- Cells* 11; 1248.
8. Huang, N., Pérez. P., Kato, T., Mikami, Y., Okuda, K., Gilmore, R.C., *et al.* (2021) SARS-CoV-2 infection of the oral cavity and saliva. *Nat. Med.* 27; 892–903.
  9. Iwasaki, S., Fujisawa, S., Nakakubo, S., Kamada, K., Yamashita, Y., Fukumoto, T., *et al.* (2020) Comparison of SARS-CoV-2 detection in nasopharyngeal swab and saliva. *J. Infect.* 81; e145–e147.
  10. Kojo, A., Yamada, K. and Yamamoto, T. (2016) Glucose transporter 5 (GLUT5)-like immunoreactivity is localized in subsets of neurons and glia in the rat brain. *J. Chem. Neuroanat.* 74; 55–70.
  11. Matuck, B. F., Dolhnikoff, M., Duarte-Neto, A. N., Maia, G., Gomes, S. C., Sendyk, D. I., *et al.* (2021) Salivary glands are a target for SARS-CoV-2: a source for saliva contamination. *J. Pathol.* 254; 239–243.
  12. Matuck, B. F., Dolhnikoff, M., Maia, G. V. A., Sendyk, D. I., Zarpellon, A., Gomes, S. C., *et al.* (2020) Periodontal tissues are tar-gets for Sars-Cov-2: a post-mortem study. *J. Oral Microbiol.* 13; 1848135.
  13. Pradeep, G. L., Uma, K., Sharada, P. and Prakash, N. (2009) Histological assessment of cellular changes in gingival epithelium in ante-mortem and post-mortem specimens. *Indian J. Dent. Res.* 1; 61–65.
  14. Rajkumari, S., Mensudar, R., Naveen, N., Thayumanavan, B. and Thammaiah, S. (2020) Estimation of postmortem death interval from autopsied tongue tissue: a cross-sectional study. *J. Oral Maxillofac. Pathol.* 24; 568–571.
  15. Reynold, E. S. (1963) The use of lead citrate at high pH as an electron-opaque stain in electron microscopy. *J. Cell Biol.* 17; 208–212.
  16. Sakaguchi, W., Kubota, N., Shimizu, T., Saruta, J., Fuchida, S., Kawata, A., *et al.* (2020) Existence of SARS-CoV-2 entry molecules in the oral cavity. *Int. J. Mol. Sci.* 21; 6000.
  17. Sawa, Y., Ibaragi, S., Okui, T., Yamashita, J., Ikebe, T. and Harada, H. (2021) Expression of SARS-CoV-2 entry factors in human oral tissue. *J. Anat.* 238; 1341–1354.
  18. Shi, Y., Wang, G., Cai, X.-P., Deng, J.-W., Zheng, L., Zhu, H.-H., *et al.* (2020) An overview of COVID-19. *J. Zhejiang Univ. Sci. B* 21; 343–360.
  19. Song, H., Seddighzadeh, B., Cooperberg, M. R. and Huang, F. W. (2020) Expression of ACE2, the SARS-CoV-2 receptor, and TMPRSS2 in prostate epithelial cells. *Eur. Urol.* 78; 296–298.
  20. Suzuki, H., Yamada, K., Matsuda, Y., Onozuka, M. and Yamamoto, T. (2017) CXCL14-like Immunoreactivity Exists in Somatostatin-containing Endocrine Cells, and in the Lamina Propria and Submucosal Somatostatinergic Nervous System of Mouse Ali-mentary Tract. *Acta Histochem. Cytochem.* 26; 50: 149–158.
  21. Tammara, A., Adebajo, G. A. R., Chello, C., Parisella, F. R., Rello, J., Del, Nonno, F., *et al.* (2020) Severe palmar hyperkeratosis and hemochezia in COVID-19. *Dermatol. Ther.* 33; e14423.
  22. Xu, H., Zhong, L., Deng, J., Peng, J., Dan, H., Zeng, X., *et al.* (2019) High expression of ACE2 receptor of 2019-nCoV on the epithelial cells of oral mucosa. *Int. J. Oral Sci.* 12; 8.

---

This is an open access article distributed under the Creative Commons Attribution-NonCommercial 4.0 International License (CC-BY-NC), which permits use, distribution and reproduction of the articles in any medium provided that the original work is properly cited and is not used for commercial purposes.

---